Observation of spin glass transition in spinel $LiCoMnO_4$*

Chen Hong(陈 红)[a], Yang Xu(杨 旭)[b], Zhang Pei-Song(张培松)[a], Liang Lei(梁 磊)[a], Hong Yuan-Ze(洪源泽)[a], Wei Ying-Jin(魏英进)[b], Chen Gang(陈 岗)[b,c], Du Fei(杜 菲)[b], and Wang Chun-Zhong(王春忠)[b,c]†

[a] College of Physics, Beihua University, Jilin 132013, China
[b] Key Laboratory of Physics and Technology for Advanced Batteries (Ministry of Education), College of Physics, Jilin University, Changchun 130012, China
[c] State Key Laboratory of Superhard Materials, Jilin University, Changchun 130012, China

(Received 1 June 2015; revised manuscript received 10 August 2015; published online 20 October 2015)

Spinel $LiCoMnO_4$ is prepared by solid-state reaction and its magnetic properties are comprehensively studied by direct current (DC) and alternating current (AC) susceptibilities, isothermal remanent magnetizations, and magnetic hysteresis. Fitting to the Curie–Weiss law by using high-temperature zero-field-cooled susceptibility confirms a low-spin state of Co^{3+} with $S = 0$. Both the fitting parameters first increase and then tend to be saturated at high magnetic fields through using isothermal remanent magnetizations, which suggests a spin glass transition at low temperature. AC susceptibility study also supports this conclusion since the frequency dependence of peak position and intensity follows the tendency of a spin glass transition. The origin of the spin-glass transition in $LiCoMnO_4$ might be attributed to a spatial segregation between non-magnetic Co^{3+} regions and spin glass ordered regions of Mn^{4+} ions.

Keywords: $LiCoMnO_4$, spin glass, DC susceptibility, AC susceptibility

PACS: 72.20.–i, 75.25.–j, 75.40.–s **DOI:** 10.1088/1674-1056/24/12/127501

1. Introduction

With the growing demand for the high-performance lithium ion batteries (LIBs), $LiMn_2O_4$ with spinel structure has attracted much attention owing to the low cost of manganese and one-dimensional Li-ion migration pathway.[1–4] $LiMn_2O_4$ crystallizes in the space group *Fd-3m*, and Li, Mn, and O occupy 8*a*, 16*d*, and 32*e* sites, respectively. Owing to the redox Mn^{3+}/Mn^{4+}, $LiMn_2O_4$ shows a reversible capacity of nearly 135 mA·h·g^{-1}.[4] However, the unsatisfactory cycle stability and voltage degradation prevent it from being further used as the potential cathode material for LIBs. Many efforts have been made to improve its electrochemical performance via partially substituting Mn by Co, Ni, Cr or Fe.[5–8]

A study on the crystallographic, electronic and magnetic structure of the cathode material is meaningful for the understanding of the electrochemical property since cation ordering and phase stability are closely related to the charge capacity and capacity retention. $LiMn_2O_4$ has been found to show a magnetic transition from paramagnetism to spin glass (SG) because of the geometrical frustration.[9] When Mn ions are partly substituted by Cr, an SG is also found in $LiCrMnO_4$ due to the random distribution of Cr^{3+} and Mn^{4+} ions.[10] $LiCoMnO_4$ is another attractive cathode material because it can provide a high voltage plateau above 5 V.[5] Electron paramagnetic resonance (EPR) spectrum of $LiCoMnO_4$ suggests a low-spin state of Co^{3+} state with $S = 0$.[11] Interestingly, if Co^{3+} ions occupy 16*d* site homogeneously, the nonmagnetic ions will act as the dilution to the magnetic interaction and paramagnetism is expected. In this paper, an SG transition is proposed in $LiCoMnO_4$ by the comprehensive magnetic method. In contrast to the expected paramagnetism, the existence of SG transition can be explained on the basis of cation random distribution in $LiCoMnO_4$.

2. Experiment

$LiCoMnO_4$ was prepared by a solid-state reaction. Stoichiometric mixtures of Li_2CO_3, Co_2O_3, and Mn_2O_3 were ground thoroughly, and fired at 650 °C or 6 h and then at 850 °C or 24 h before cooling to room temperature naturally. The crystal structure of the as-prepared sample was studied by x-ray diffraction (XRD) in capillary transmission mode on a STOE STADI P diffractometer with Mo Kα_1 radiation. Diffraction data were recorded over a 2θ range of 5°–80° in steps of 0.01°. The software Fullprof was used for data analysis and Rietveld refinement of the structural model. Magnetic characterization was performed by a superconducting quantum interference device magnetometer (Quantum Design MPMS-XL).

3. Results and discussion

Figure 1 shows the XRD pattern for the as-prepared $LiCoMnO_4$. Rietveld refinement confirms the spinel structure

*Project supported by the National Key Basic Research Program of China (Grant No. 2015CB251103), the Development Program of Science and Technology of Jilin Province, China (Grant No. 20140101093JC), and the Program of Science and Technology of Jilin City, China (Grant No. 201434006).

†Corresponding author. E-mail: wcz@jlu.edu.cn

© 2015 Chinese Physical Society and IOP Publishing Ltd

with space group of Fd-3m and no impurity phase can be detected. Detailed refinement parameters are listed in Table 1. Note that the relative intensities of (311) and (400) peaks are different from those of $LiMn_2O_4$,[12] which may come from the Td and 16c defects due to the random distributions of $Mn^{4+}$and Co^{3+} ions at the 8a and 16c sites, respectively. The degrees of Td and 16c defects are calculated to be 14.9% and 0.9%, respectively, by means of the Rietveld refinement.

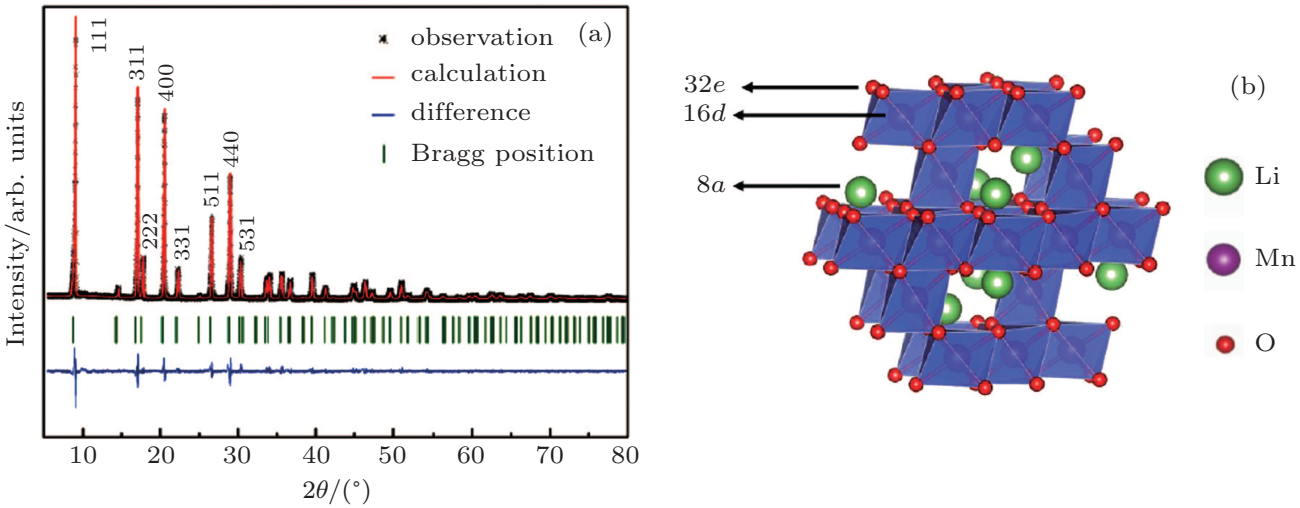


Fig. 1. (color online) (a) Observed and calculated x-ray diffraction profiles together with their difference for the as-prepared $LiCoMnO_4$ compound; (b) Schematic diagram for the crystal structure of spinel $LiMn_2O_4$.

Table 1. $LiCoMnO_4$ crystal structure parameters determined by Rietveld refinement.

Atom	Wyckoff position	x	y	z	Occupancy
Li	8a	0.12500	0.12500	0.12500	0.85056
Mn	8a	0.12500	0.12500	0.12500	0.07472
Co	8a	0.12500	0.12500	0.12500	0.07472
Li_2	16d	0.50000	0.50000	0.50000	0.07472
Mn_2	16d	0.50000	0.50000	0.50000	0.45802
Co_2	16d	0.50000	0.50000	0.50000	0.45802
Mn_3	16c	0.00000	0.00000	0.00000	0.00462
Co_3	16c	0.00000	0.00000	0.00000	0.00462
O	32e	0.26204	0.26204	0.26204	1.00000

Space group: Fd-3m Lattice constant: $a = 8.07309$, $R_{wp} = 12.2$, $R_{exp} = 9.93$, $R_f = 4.06$.

XPS spectra were carried out to further study the valence states of Co and Mn ions as shown in Fig. 2. In the Co 2p spectrum, the binding energies of the peaks located at 780.2 eV and 795.2 eV correspond to $2p_{3/2}$ and $2p_{1/2}$of Co^{3+}, in accordance with those reported in $LiCoO_2$, along with two satellite peaks at 790.1 eV and 805.3 eV.[13] In the Mn 2p spectrum, the peak located at 642.5 eV agrees with the $2p_{3/2}$ of Mn^{4+} as reported in Ref. [14].

Zero-field cooled (ZFC) and field-cooled (FC) susceptibilities from 5 K to 300 K under an applied field of 1000 Oe (1 Oe = 79.5775 A·m^{-1}) are exhibited in Fig. 3 with the inverse susceptibility curve as indicated in the inset. At high-T, the susceptibility increases with the decrease of temperature, indicating a paramagnetic behavior. By fitting the Curie-Weiss law using high-temperature paramagnetic data, Curie and Weiss constants are calculated to be $C = 1.84$ emu·K/mol·Oe and $\theta = -49(1)$ K, respectively. The negative Weiss constant indicates the antiferromagnetic interaction between spins in $LiCoMnO_4$. By employing the equation $C = N\mu_{eff}^2/3k_B$, where N is the molar concentration of ions and μ_B is the Bohr magneton, the experimental effective moment μ_{eff}^{exp} is calculated to be 3.83(2) μ_B. On the other hand, the theoretical effective moment μ_{eff}^{theo} should come from the contribution of Mn^{4+} ions ($S = 3/2$), since Co^{3+} ions are suggested to be in the low-spin state in the octahedral coordination by ESR measurements with six 3d electrons in three t_{2g} orbits, $S = 0$.[15] Hence the theoretical effective moment of $LiCoMnO_4$ is calculated to be 3.87 μ_B via $\mu_{eff}^{theo} = 2\sqrt{S(S+1)}\mu_B$, where S equals the spin quantum of Mn^{4+} ($S = 3/2$). The obtained value is consistent with the experimental effective moment of $LiCoMnO_4$.

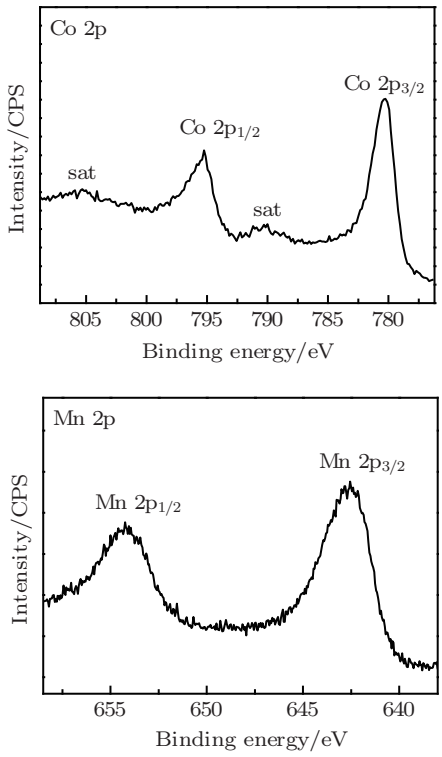


Fig. 2. Co 2p and Mn 2p XPS of $LiCoMnO_4$.

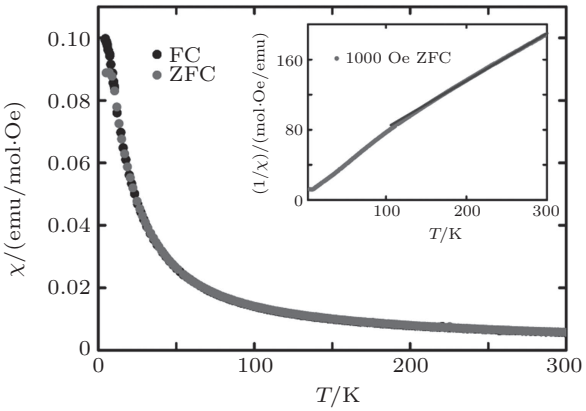


Fig. 3. ZFC/FC curves of $LiCoMnO_4$ under 1000 Oe and reciprocal ZFC curve with the Curie–Weiss fitting in inset.

At low-T, ZFC and FC curves begin to show an irreversible behavior at nearly 17 K, and ZFC branch displays a peak at 7 K, which is defined as the freezing temperature (T_f), reminiscence of an SG transition. To confirm the SG transition, the isothermal remanent magnetizations (M_{IRM}) are recorded and shown in Fig. 4. Applying a procedure in which the sample is zero-field cooled to 5 K and different magnetic fields are applied for 10 min, a slow decay of the M_{IRM} after the field is reduced to zero, which is a typical feature for the spin glass behavior below T_f.[16] By fitting the time dependence of magnetization using the formula $M_{IRM}(t) = M_0 - \alpha \ln(t)$, we can obtain the fitting parameters M_0 and α as a function of magnetic field (the inset of Fig. 4). Both the parameters first increase and then tend to saturate at high magnetic fields, which is a typical feature for SG system.[17]

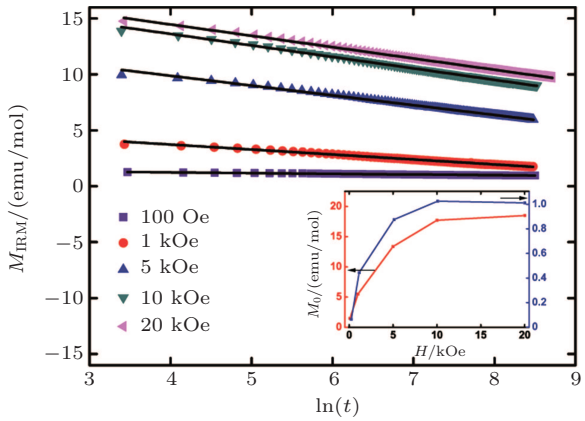


Fig. 4. (color online) Plots of isothermal remanent magnetization versus natural logarithm of time at different applied magnetic fields, and plots of fitting parameters M_0 and α in fitting formula $M_{IRM}(t) = M_0 - \alpha \ln(t)$ versus magnetic field (in inset).

The dynamic behavior of SG near T_f is also studied, and AC susceptibilities under different frequencies ranging from 1 Hz to 500 Hz are shown in Fig. 5. The height of the peak decreases and the peak position shifts toward the high temperature with the increase of frequency, in accordance with the characteristics of SG behavior. Supposing the existence of an equilibrium phase transition with a divergence of relaxation time (τ) near the transition temperature, we employ the power law to explain the relaxation behavior in the SG system. The power law can be described as $\tau = \tau_0(T_f/T_g - 1)^{-zv}$, where T_g corresponds to the relaxation temperature, τ_0 is related to the relaxation time of the individual magnetic moment, and zv is the dynamic critical exponent.[18] The values are calculated to be $\tau_0 = 6.2 \times 10^{-11}$ s and $zv = 6.9$, which fall in the typical values ($zv \sim 7.9 \pm 1$ K) determined by the simulations of Ogielski for a three-dimensional SG with short-range magnetic interactions.[19] This also confirms the SG transitions in spinel $LiCoMnO_4$.

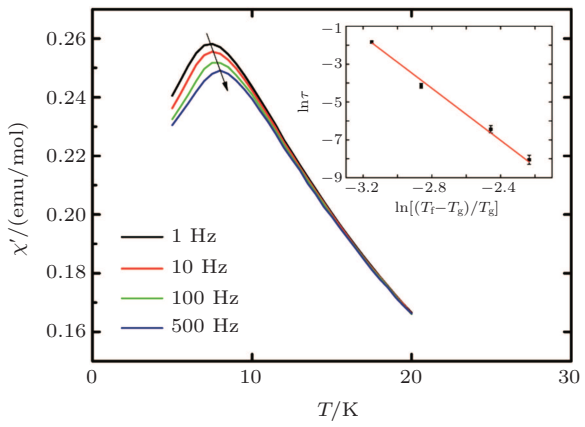


Fig. 5. (color online) Temperature dependences of the real-part of AC susceptibility in the frequency range from 1 Hz to 500 Hz, and the fitting to power law (in inset).

The field dependences of magnetizations (Fig. 6(a)) under different temperatures are recorded, with the magnified curves indicated in the inset. The magnetization shows a linear dependence on magnetic field at 50 K. The small magnetic hysteresis appears as temperature decreases below T_{irr}. The coercive field and remanence at 5 K are -201 Oe and 3.4×10^{-3} μ_B/Mn, respectively. Note that there is no magnetic saturation at 5 K even under a strong field (5 T), which is consistent with the competition nature between antiferromagnetic and ferromagnetic interaction for SG. The Arrott plot (Fig. 6(b)), obtained from magnetization isotherms, shows strong curvature toward the H/M axis without any intercept on the M^2 axis, indicating no sign of the spontaneous magnetization.[20]

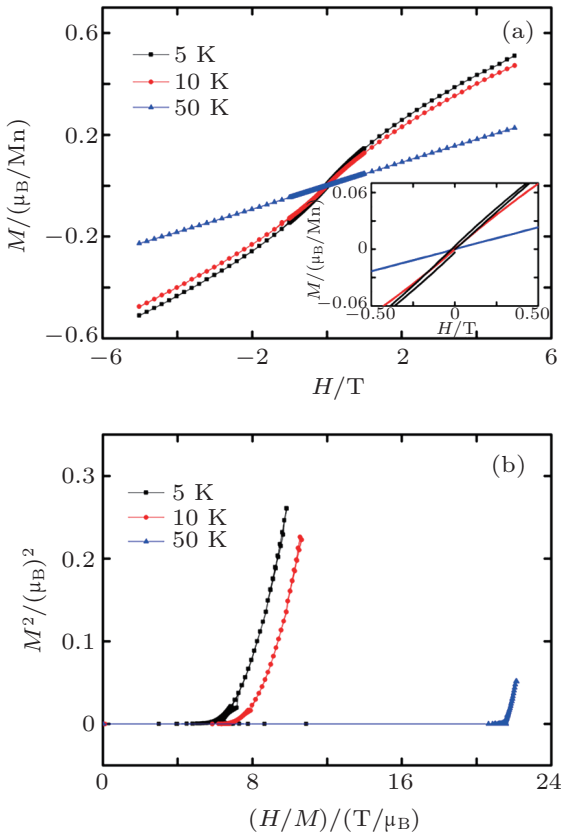


Fig. 6. (color online) (a) Variations of magnetic field and magnification of specified parts (in inset) with magnetization and (b) Arrott plots (H/M versus M^2), at different fixed temperatures of $LiCoMnO_4$.

Note that the geometrical frustration and disorder are two major reasons for the formation of SG. In the spinel $LiMn_2O_4$, the tetrahedral arrangement of Mn ions with the same bond distance would give a strong frustration effect and frustration parameter (f) equals 11. Correspondingly, an SG transition is observed in $LiMn_2O_4$ with $T_f = 25$ K.[9] When Mn ions are partly substituted by Cr, an SG is also suggested, but f_{Cr} is lower than 10,[10] which is considered as the critical value at which the geometrical frustration plays an effect. This means that the frustrated tetrahedral arrangement of Mn ions would be destroyed when Cr^{3+} ions are introduced into the lattice. The random distributions of Cr^{3+} and Mn^{4+} ions are likely to be responsible for the formation of SG. Usually, nonmagnetic ions act as the dilution to the magnetic interaction, and the doped compounds show paramagnetism. In $LiCoMnO_4$, if the random distributions of Co^{3+} and Mn^{4+} ions are homogeneous, nonmagnetic Co^{3+} ions would destroy the exchange interaction between Mn^{4+} ions and paramagnetism is expected in the whole measured T region. But, interestingly, $LiCoMnO_4$ shows an SG transition like $LiCrMnO_4$, instead of the expected paramagnetism, and the frustration parameter equals 7, which also implies that nonmagnetic Co^{3+} ions destroy the frustrated lattice. The random distributions of Co^{3+} and Mn^{4+} ions are likely to result in the formation of different ions clusters due to the different electronic structures between Mn^{4+} ions ($e_g^0t_{2g}^3$, $S = 3/2$) and Co^{3+} ions ($e_g^0t_{2g}^6$, $S = 0$). Furthermore, it should be addressed that the differences in preparation method and sintered temperature would induce the difference in the valence state of ions, short-range structural disorder and formation of clusters, especially in the doped materials, which determine the physical and electrochemical properties. For example, the magnetic parameters of layered $LiNi_{0.4}Mn_{0.4}Co_{0.2}O_2$ show a strong dependence on the preparation method, and the magnetic ground state ranges from SG to cluster-SG.[21–23] Therefore, how to obtain an ideal $LiCoMnO_4$ with controlled ion disorder might be a tough question, which needs more studies in future.

4. Conclusions

We study the structural and magnetic properties of $LiCoMnO_4$ by Rietveld analysis and DC and AC susceptibilities. The fitting to the high-temperature Curie–Weiss law suggests the low spin state of Co^{3+} ions. The spin glass transition at low temperature is confirmed by the irreversibility between ZFC and FC curve, the isothermal remanent magnetizations, and the fitting to the AC susceptibility peak by using the power law. The origin of SG is attributed to spatial segregation between non-magnetic Co^{3+} clusters and spin glass ordered regions of Mn^{4+} clusters rather than geometrical frustration.

References

[1] Kim D K, Muralidharan P, Lee H, Ruffo R, Yang Y, Chan C K, Peng H, Huggins R A and Cui Y 2008 *Nano Lett.* **8** 3948
[2] Belharouak I, Sun Y, Lu W and Aminea K 2007 *J. Electrochem. Soc.* **154** A1083
[3] Lee H W, Muralidharan P, Ruffo R, Mari C M, Cui Y and Kim D K 2010 *Nano Lett.* **10** 3852
[4] Sun Y K, Oh I H and Kim K Y 1997 *Ind. Eng. Chem. Res.* **36** 4839
[5] Kawai H, Nagata M, Tukamoto H and West A R 1998 *Electrochem. Solid ST.* **1** 212
[6] Arrebola J C, Caballero A, Cruz M, Hernan L, Morales J and Castellon E R 2006 *Adv. Funct. Mater.* **16** 1904
[7] Nikolowski K, Bramnik N N and Ehrenberg H 2008 *Ionics* **14** 121

[8] Shigemura H, Sakaebe H, Kageyama H, Kobayashi H, West A R, Kanno R, Morimoto S, Nasu S and Tabuchia M 2001 *J. Electrochem. Soc.* **148** A730
[9] Xin X G, Shen J Q and Shi S Q 2012 *Chin. Phys. B* **21** 0128202
[10] Arillo M A, Cuellob G, Lopeza M L, Martina P, Picoa C and Veigaa M L 2005 *Solid State Sci.* **7** 25
[11] Stoyanova R K, Zhecheva E N and Gorova M Y 2000 *J. Mater. Chem.* **10** 1377
[12] Akimoto J, Takahashi Y, Gotoh Y and Mizuta S 2000 *Chem. Mater.* **12** 3246
[13] Daheron L, Martinez H, Dedryvere R, Baraille I, Menetrier M, Denage C, Delmas C and Gonbeau D 2009 *J. Phys. Chem. C* **113** 5843
[14] Dou S and Wang W 2011 *J. Solid State Electrochem.* **15** 399
[15] Ropka Z and Radwanski R J 2003 *Phys. Rev. B* **67** 172401
[16] Wang BS, Tong P and Sun Y P 2010 *Appl. Phys. Lett.* **97** 042508
[17] Bie X, Wei Y, Liu L, Nikolowski K, Ehrenberg H, Chen H, Wang C, Chen G and Du F 2013 *J. Alloys Compd.* **551** 37
[18] Liu L, Bie X, Ehrenberg H, Wang C, Wei Y, Chen G and Du F 2011 *J. Appl. Phys.* **110** 093912
[19] Ogielski A T 1985 *Phys. Rev. B* **32** 7384
[20] Du F, Huang Z, Wang C, Meng X and Chen G 2007 *J. Appl. Phys.* **102** 113906
[21] Bie X, Liu L, Ehrenherg H, Wei Y, Nikolowski K, Wang C, Ueda Y, Chen H, Chen G and Du F 2012 *RSC Adv.* **2** 9986
[22] Rui W B, He M C, You B, Shi Z, Zhou S M, Xiao M W, Gao Y, Zhang W, Sun L and Du J 2014 *Chin. Phys. B* **23** 107502
[23] Zhang K C and Song P Y 2010 *Chin. Phys. B* **19** 097105